IFAC-PapersOnLine, Volume 49, Issue 17, 2016, pp. 308-313
20th IFAC Symposium on Automatic Control in Aerospace, ACA 2016,
21-25 August 2016, Sherbrooke, Quebec, Canada.
DOI:10.1016/j.ifacol.2016.09.053

Adaptive Control with Neural Networks-based Disturbance Observer for a Spherical UAV

Tommaso Matassini * **Hyo-Sang Shin** ** **Antonios Tsourdos** *** **Mario Innocenti** ****

* *Università di Pisa, Italy, (e-mail: matassini.tommaso@gmail.com)*
** *Cranfield University, UK (e-mail: h.shin@cranfield.ac.uk)*
*** *Cranfield University, UK (e-mail: a.tsourdos@cranfield.ac.uk)*
**** *Università di Pisa, Italy, (e-mail: mario.innocenti@unipi.it)*

Abstract: This paper develops a control scheme for a Spherical Unmanned Aerial Vehicle (UAV) which can be used in complex scenarios where traditional navigation and communications systems would not succeed. The proposed scheme is based on the nonlinear control theory combined with Adaptive Neural-Networks Disturbance Observer (NN-DOB) and controls the attitude and altitude of the UAV in presence of model uncertainties and external disturbances. The NN-DOB can effectively estimate the uncertainties without the knowledge of their bounds and the control system stability is proven using Lyapunov's stability theorems. Numerical simulation results demonstrate the validity of the proposed method on the UAV under model uncertainties and external disturbances.

Keywords: Spherical UAV, model uncertainties and external disturbances, disturbance observer, adaptive control, neural networks.

1. INTRODUCTION

Recent researches (Gui et al. [2015],Mizutani et al. [2015]) have proposed the design of 'spherical-like' UAVs. In this article the focus is about a coaxial, flap actuated, spherical helicopter, developed in Cranfield University with the specific purpose of exploration and exploitation of complex environments (Dixon and Fernandez [2013]).

The spherical frame provides protection to the inner components of the UAV and allows to roll along the floor if the environment permits. The coaxial motors provide as much thrust as possible in the small volume of the sphere and allow yaw control through differential propeller speed. The flaps, placed below the propellers, allow a decoupled roll and pitch control in a thrust vectoring manner. The final result of this design is a well-protected, compact, easily controlled, flexible and agile UAV for operations in complex environments.

As in the spherical UAV, system identification is quite challenging in small and unconventional airframes. Modelled dynamics of such an airframe often contain uncertainties. Moreover, small external disturbances could become severe since they might be relatively strong to such a platform, unlike to relatively large and conventional aircraft. Therefore, when designing a flight control system for small and/or unconventional UAVs, incorporating uncertainties and disturbances is of great importance.

This paper aims to develop a control system for the spherical UAV, which is able to cope with model uncertainties and external disturbances. In order to achieve this aim, we propose an adaptive control system with Neural Network-Disturbance Observer. The proposed approach adjusts rotor speed and flap angles to control attitude and altitude of the spherical UAV.

The basic control system is designed based on the Lyapunov control theory. NN-DOB adaptively estimates model uncertainties and external disturbances and these estimates are incorporated in the original control commands obtained from the Lyapunov control theory. The stability of the entire system is analytically investigated. The analysis results confirm that the proposed control system guarantees the stability of entire system under the presence of uncertainties and disturbances, even without knowledge of their bounds.

The main advantage of the proposed control method is the applicability to every rigid (DoF) body in which forces and torques can be applied.

This paper is organised as follows: Section 2 introduces the notations used throughout this paper and describes the dynamic model of the spherical UAV. Sections 3 explains the proposed control method for a single integrator system and its most useful extensions. Section 4 describes the application of the proposed control method on the spherical UAV. Control performance of the proposed method is demonstrated via numerical simulations in Section 5 and, finally, Section 6 presents the conclusions.

2. MODELING

The final design of the spherical UAV is shown in Fig. 1; the body-fixed frame $B = \{x_b, y_b, z_b\}$, is located in the Body Axis Centre (BAC), which is the geometric centre of

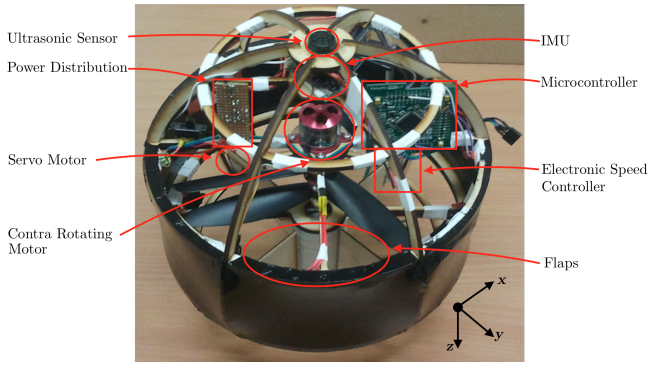

Fig. 1. UAV Prototype developed in Cranfield University.

symmetry; the axes directions are shown in the left bottom corner.

2.1 Actuation principles

The actuation system is composed of two contra-rotating motors along z-axis and provides a force F and a torque τ; the relation with the PWMs is found with a test rig.

$$F = f_1(\text{PWM}_1, \text{PWM}_2)\frac{1}{1+\tau_m s} \tag{1}$$

$$\tau = f_2(\text{PWM}_1, \text{PWM}_2)\frac{1}{1+\tau_m s} \tag{2}$$

where τ_m represents a first order time constant and f_1 and f_2 are nonlinear function of both PWM_1 and PWM_2 .

Define $[X\ Y\ Z]^T_{Act}$ as the applied forces and $[L\ M\ N]^T_{Act}$ as the applied torques in the body frame B. The two flaps make the UAV behave as a thrust vectored nozzle; the force F produced by the motors is steered in three dimensions due to the flap angles α_1 and α_2:

$$\begin{bmatrix} X \\ Y \\ Z \end{bmatrix}_{Act} = \begin{bmatrix} F_x \\ F_y \\ F_z \end{bmatrix} = \frac{1}{\sqrt{c^2_{\alpha_1} s^2_{\alpha_2} + c^2_{\alpha_2}}} \begin{bmatrix} -c_{\alpha_1} s_{\alpha_2} \\ +s_{\alpha_1} c_{\alpha_2} \\ -c_{\alpha_1} c_{\alpha_2} \end{bmatrix} F \tag{3}$$

From now on we define $c_x = \cos x$, $s_x = \sin x$ and $t_x = \tan x$ for the simplicity of the notation. L and M torques are generated because the forces X and Y are applied in a point on the z-axis, d_V below the BAC.

$$\begin{bmatrix} L \\ M \\ N \end{bmatrix}_{Act} = \begin{bmatrix} 0 \\ 0 \\ d_V \end{bmatrix} \times \begin{bmatrix} F_x \\ F_y \\ F_z \end{bmatrix} + \begin{bmatrix} 0 \\ 0 \\ \tau \end{bmatrix} = \begin{bmatrix} -d_V F_y \\ +d_V F_x \\ \tau \end{bmatrix} \tag{4}$$

Merging (3) and (4), the actuators action is shown in (5):

$$\begin{bmatrix} X \\ Y \\ Z \\ L \\ M \\ N \end{bmatrix}_{Act} = \begin{bmatrix} F_x \\ F_y \\ F_z \\ -d_V F_y \\ +d_V F_x \\ \tau \end{bmatrix} \frac{1}{\tau_m s + 1} \tag{5}$$

2.2 Dynamics

Consider the motion of the body-fixed frame B about an Earth-fixed reference frame $E = \{x_e, y_e, z_e\}$. There are two assumptions: first, the body is assumed to be rigid; second, the Earth is flat and E is considered inertial. The frame E is selected with the North-East-Down (NED) configuration.

From the Newton-Euler equations, it holds:

$$\begin{bmatrix} X \\ Y \\ Z \end{bmatrix} = m \begin{bmatrix} \dot{u} \\ \dot{v} \\ \dot{w} \end{bmatrix} + m \begin{bmatrix} p \\ q \\ r \end{bmatrix} \times \begin{bmatrix} u \\ v \\ w \end{bmatrix} \tag{6}$$

$$\begin{bmatrix} L \\ M \\ N \end{bmatrix} = I_B \begin{bmatrix} \dot{p} \\ \dot{q} \\ \dot{r} \end{bmatrix} + \begin{bmatrix} p \\ q \\ r \end{bmatrix} \times I_B \begin{bmatrix} p \\ q \\ r \end{bmatrix} \tag{7}$$

where m is the UAV mass, I_B is the Inertia matrix in the body frame B, $v_B = [u\ v\ w]^T$ is the linear velocity in B, $\omega = [p\ q\ r]^T$ is the angular velocity in B, $\mathbf{F} = [X\ Y\ Z]^T$ are the applied forces in B and $\mathbf{T} = [L\ M\ N]^T$ are the applied torques in B. $\mathbf{F}$ and$\mathbf{T}$ include gravity contribution and external disturbances.

The relation between the body-fixed angular velocity ω and the Euler angles derivatives, $\dot{\eta} = \left[\dot{\phi}\ \dot{\theta}\ \dot{\psi}\right]^T$, is determined writing the body rates components into the inertial frame:

$$\dot{\eta} = \begin{bmatrix} 1 & s_\phi t_\theta & c_\phi t_\theta \\ 0 & c_\phi & -s_\phi \\ 0 & \frac{s_\phi}{c_\theta} & \frac{c_\phi}{c_\theta} \end{bmatrix} \omega = J\omega \tag{8}$$

Therefore, using the Direct Cosine Matrix (DCM), the linear velocities in the reference frame are computed as:

$$v_E = \frac{d}{dt}\begin{bmatrix} P_N \\ P_E \\ P_D \end{bmatrix} = DCM^T v_B \tag{9}$$

The integration of (8) and (9) with the proper initial condition makes the position and attitude of the UAV known. For more details, see Stevens et al. [2015].

3. ADAPTIVE CONTROL LAW DESIGN

The proposed control system considers the system dynamics as a single integrator system:

$$\dot{x} = k \cdot u + D(x, u, t) \tag{10}$$

where x is the state to be controlled, k is a known constant and $D(x, u, t)$ denotes a disturbance. Note that model uncertainties, external disturbances and/or neglected dynamics are incorporated in the disturbance, $D(x, u, t)$. The aim of the control law is to make x follow a desired command x_C. Define the tracking error as

$$e = x_C - x \tag{11}$$

Define a positive definite Lyapunov function

$$V_1 = \frac{1}{2}e^2 \tag{12}$$

The derivative of V_1 is

$$\dot{V}_1 = e\dot{e} = e(\dot{x}_C - \dot{x}) = e(\dot{x}_C - k \cdot u - D(x, u, t)) \tag{13}$$

This mean that, if we could choose

$$u^* = \frac{1}{k}(\dot{x}_C - D(x, u, t) + \alpha e), \quad \alpha > 0 \tag{14}$$

We could obtain

$$\dot{V}_1^* = -\alpha e^2 \tag{15}$$

Which is negative definite. In practice, the uncertainty $D(x, u, t)$ is (obviously) unknown, and it is also difficult to know an upper bound $\bar{D}$ that achieves

$$\|D(x, u, t)\| < \bar{D} \quad \forall x, u, t$$

For that reason an online adaptive observer is proposed for the estimation of D. The proposed control law achieves the

tracking of the command x_C along with the estimation of the uncertainty.

3.1 Disturbance Estimation

The NN-DOB is implemented with a Radial Basis Function Neural Network (RBF-NN), which has an efficient capacity for approximating nonlinear dynamics; see Lavretsky and Wise [2012] for more details. The NN-DOB estimator has an input layer, a hidden layer and an output layer, as shown in Fig. 2.

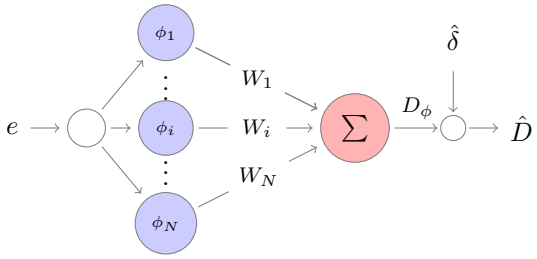

Fig. 2. RBF-NN structure.

The hidden layer is composed of N neurons, each one with a centre, μ_i, and a width, σ_i. Each hidden node contains a RBF, a nonlinear function satisfying $\phi(x) = \phi(\|x\|)$. The output depends only on the distance from the center, scaled by the width:

$$\phi_i(e) = f(\|\frac{e-\mu_i}{\sigma_i}\|) \tag{16}$$

The most used RBF are gaussian, logarithmic and multiquadric functions. The output layer is computed using the following weighted sum:

$$D_\phi = \sum_{i=1}^{N} W_i\phi_i(e) = \mathbf{W}^T\mathbf{\Phi} \tag{17}$$

where W_i is the weight between the i^{th} hidden neuron and the output, $\mathbf{W} = [W_1 \ \cdots \ W_N]^T$ and $\mathbf{\Phi} = [\phi_1 \ \cdots \ \phi_N]^T$. Define δ as the minimum estimation error between the real disturbance and D_ϕ and $\mathbf{W}^*$ as the weight vector that achieves the minimum δ:

$$\mathbf{W}^* = \arg\min_{\mathbf{W}}(\|D - D_\phi\|) \tag{18}$$

So that

$$D(x,u,t) = D_\phi(\mathbf{W}^*) + \delta = \mathbf{W}^{*T}\mathbf{\Phi} + \delta \tag{19}$$

The estimation error δ and the optimal weight $\mathbf{W}^*$ are unknown, so the total disturbance D is estimated as

$$\hat{D} = \mathbf{W}^T\mathbf{\Phi}(e) + \hat{\delta} \tag{20}$$

Where $\mathbf{W}$ and $\hat{\delta}$ are calculated through an adaptive law.

3.2 Control Law

Define the Lyapunov function

$$V_2 = V_1 + \frac{1}{2\eta_1}(\mathbf{W}^* - \mathbf{W})^T(\mathbf{W}^* - \mathbf{W}) + \frac{1}{2\eta_2}(\delta - \hat{\delta})^2 \tag{21}$$

This function V_2 can be rewritten as $V_2 = \frac{1}{2}z^TPz$, where

$$z = \begin{bmatrix} e \\ \mathbf{W}^* - \mathbf{W} \\ \delta - \hat{\delta} \end{bmatrix}, \quad P = diag\left\{1, \frac{1}{\eta_1}\mathrm{I}_{N\times N}, \frac{1}{\eta_2}\right\} \tag{22}$$

Note that V_2 is positive definite with respect to the variable z, and not only w.r.t the error e. The derivative of V_2 is

$$\dot{V}_2 = e\dot{e} + \frac{1}{\eta_1}(\mathbf{W}^* - \mathbf{W})^T(\dot{\mathbf{W}}^* - \dot{\mathbf{W}}) + \frac{1}{\eta_2}(\delta - \hat{\delta})(\dot{\delta} - \dot{\hat{\delta}}) \tag{23}$$

For every disturbance the couple $(\mathbf{W}^*, \delta)$ is fixed, so we can assume

$$\dot{\mathbf{W}}^* = 0 \tag{24}$$

$$\dot{\delta} = 0 \tag{25}$$

Substituting (13), (24) and (25) into (23) yields

$$\dot{V}_2 = e(\dot{x}_C - k\cdot u - D) - \frac{1}{\eta_1}(\mathbf{W}^* - \mathbf{W})^T\dot{\mathbf{W}} - \frac{1}{\eta_2}(\delta - \hat{\delta})\dot{\hat{\delta}} \tag{26}$$

Design the adaptive law as

$$\dot{\mathbf{W}} = -\eta_1 \ \mathbf{\Phi} \ e \tag{27}$$

$$\dot{\hat{\delta}} = -\eta_2 \ e \tag{28}$$

Design the control action as

$$u = \frac{1}{k}(\alpha e + \dot{x}_C - \hat{D}) \tag{29}$$

where $\hat{D}$ is calculated from (20) and α, η_1, η_2 are positive tuning parameters. Substituting (27), (28) and (29) into (26) yields

$$\begin{aligned} \dot{V}_2 &= e(-\alpha e + \hat{D} - D) + (\mathbf{W}^* - \mathbf{W})^T\mathbf{\Phi}e + (\delta - \hat{\delta})e \\ &= -\alpha e^2 \end{aligned} \tag{30}$$

This control action makes the derivative of V_2 only negative *semi* definite, and for that reason the stability is checked with the Barbalat's Lemma. Define $\ddot{V}_2$ as:

$$\ddot{V}_2 = -2\alpha e\dot{e} = -2\alpha e(-\alpha e + \hat{D} - D) \tag{31}$$

Since e, u, $\hat{D}$, D are all bounded, then $\ddot{V}_2$ is bounded, hence $\dot{V}_2$ is uniformly continuous. Combined with the fact that V_2 is bounded from below and $\dot{V}_2$ is negative semi-definite, then it infers that $\dot{V}_2 \to 0$ as $t \to \infty$.

3.3 Estimation Direction

The disturbance equation (19) can be rewritten as

$$D = \mathbf{W}^{*T}\mathbf{\Phi}(e) + \delta = \begin{bmatrix}\mathbf{\Phi}^T & 1\end{bmatrix}\begin{bmatrix}\mathbf{W}^* \\ \delta\end{bmatrix} = \mathbf{p}^TL^* \tag{32}$$

Where $L^* = \begin{bmatrix}\mathbf{W}^* \\ \delta\end{bmatrix}$ and $\mathbf{p}^T = \begin{bmatrix}\mathbf{\Phi}^T & 1\end{bmatrix}$ is the linear map between L^* and D. Note that $\mathbf{p}^T \in \mathbb{R}^{1\times(N+1)}$, so its kernel has rank

$$rank(\ker(\mathbf{p}^T)) = N \tag{33}$$

All L who get the correct disturbance estimation are in $\mathcal{L}$:

$$\mathcal{L} = \{L | L = L^* + L_{ker}, \ L_{ker} = span\ker(\mathbf{p}^T)\} \tag{34}$$

The estimation is perfect if L reaches the set $\mathcal{L}$. The adaptive law (27) and (28) can be written as

$$\dot{L} = -\begin{bmatrix}\eta_1\mathbf{\Phi} \\ \eta_2\end{bmatrix}e, \quad L(0) = L_0 \tag{35}$$

Note that if $\eta_1 = \eta_2 = \eta$, the estimation action is

$$\dot{L} = -\eta e\mathbf{p}, \quad L(0) = L_0 \tag{36}$$

From the basic algebra theorem,

$$Im(\mathbf{p}) \perp \ker(\mathbf{p}^T) \tag{37}$$

The estimation update is perpendicular to $\mathcal{L}$, so it is made in the fastest direction and the set of weights reachable from L_0 is $L_{nearest}$, as shown in Fig. 3.

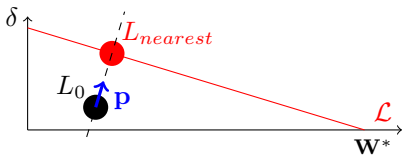

Fig. 3. The variation of the disturbance estimation is perpendicular to $\mathcal{L}$.

3.4 Advantages of the proposed control action

As written in (29), the control action is

$$u = \frac{1}{k}(\dot{x}_C + \alpha e - \hat{D})$$

It is straightforward to understand that the control action is composed by three terms: a proportional action, a Feed Forward and an estimation of the disturbance. Moreover, this kind of control doesn't act like a Sliding Mode Control, so there is no chattering in the control action.

This characteristic generalizes the control structure, as it can be applied to any system that acts as a single integrator.

3.5 Non-Linear MIMO Extension

The control laws (27), (28) and (29) can be extended to every Non-Linear, Multi Input Multi Output affine-in-the-control (NL-MIMO-AC) system whose input-to-state map $g(\mathbf{x})$ has rank bigger than the state dimension. Consider the following dynamic system:

$$\dot{\mathbf{x}} = f(\mathbf{x}) + g(\mathbf{x})u + D \qquad (38)$$
$$\mathbf{x} \in \mathbb{R}^N, D \in \mathbb{R}^N, u \in \mathbb{R}^M$$

where $M \geq N$; if the map $g(\mathbf{x}) : \mathbb{R}^M \rightarrow \mathbb{R}^N$ has always rank $\geq N$ there exist an inverse function for every state $\mathbf{x}$.

$$rank\ g(\mathbf{x}) \geq N \rightarrow \forall \mathbf{x}\ \exists\ g^{-1}(\mathbf{x}) \qquad (39)$$

Note that if $M > N$ the pseudo-inverse function $g(\mathbf{x})^\dagger = (g(\mathbf{x})^T g(\mathbf{x}))^{-1} g(\mathbf{x})^T$ can be used instead of the inverse. Rather, given the system (38) and condition (39) holds, the control action that makes $e = 0$ a stable equilibrium is

$$u = g^{-1}(\mathbf{x})(-f(\mathbf{x}) + \dot{\mathbf{x}}_C + \alpha e - \hat{D}) \qquad (40)$$

4. SPHERICAL UAV APPLICATION

The proposed control law is applied to the Spherical UAV by computing the desired control effort with (29),(40) and resolving the control allocation problem linearizing (5).

4.1 Single Integrator and Non Linear Control

The linear control law (29) can be applied to the motion equations (6), (7) because the inputs are directly integrated. From (6), the relation between $\mathbf{F}$ and v_B is similar to a single integrator.

$$\frac{d}{dt}v_B = \frac{1}{m}\mathbf{F} - \omega \times v_B \approx k \cdot u + D \qquad (41)$$

Likewise, from (7) the relation between $\mathbf{T}$ and ω is similar to a single integrator.

$$\frac{d}{dt}\omega = I_B^{-1}(\mathbf{T} - \hat{\omega} I_B \omega) = I_B^{-1}\mathbf{T} - I_B^{-1}\hat{\omega} I_B \omega \approx k \cdot u + D \qquad (42)$$

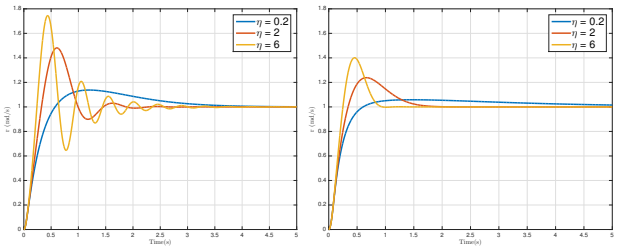

Fig. 4. Step response, r channel. Left: α=6, Right: α=15.

For example, the x-axis law

$$X = m\dot{v}_x + m(-r \cdot v_y + q \cdot v_z) \qquad (43)$$

Is equal to (10) with the change of variables $x = v_x$, $k = \frac{1}{m}$, $u = X$ and $D = r \cdot v_y - q \cdot v_z$.

Similarly, the Non Linear control law (40) can be applied to the UAV when the input variables are $\mathbf{F}$ and T and the regulated variables are the linear and angular velocities in the Earth frame v_B and $\dot{\eta}$. The demonstration that these systems are NL-MIMO-AC is made in Appendix A and B.

4.2 Commanded Variables and Control Allocation

The chosen control logic in this paper is the control of UAV altitude and attitude, so the selected variables, depending of the data available from the sensors, are x_{Int} or x_{NL}. The plant can be considered as a 'Single-Integrator'-like system if the state variables are x_{Int}, while it can be seen as a NL-MIMO-AC when the state variables are x_{NL}. In both case, the commanded variables are u_C, as shown in (44).

$$u_C = \begin{bmatrix} Z \\ L \\ M \\ N \end{bmatrix}, \quad x_{Int} = \begin{bmatrix} w \\ p \\ q \\ r \end{bmatrix}, \quad x_{NL} = \begin{bmatrix} \dot{P}_D \\ \dot{\phi} \\ \dot{\theta} \\ \dot{\psi} \end{bmatrix} \qquad (44)$$

Given u_C, the control allocation problem consists in finding the set of inputs $u_R = [F\ \tau\ \alpha_1\ \alpha_2]^T$ that reach the closest desired command (in norm). This is done linearizing and inverting equation (5), $f(u_R)$, around the current set of real input u_{R_0}.

$$u_C = f(u_R) \approx f(u_{R_0}) + \frac{\partial f}{\partial u_R}|_{u_{R_0}}(u_R - u_{R_0}) \qquad (45)$$

Inverting (45) yields

$$u_R = u_{R_0} + \left[\frac{\partial f}{\partial u_R}|_{u_{R_0}}\right]^{-1}(u_C - f(u_{R_0})) \qquad (46)$$

Note that the Jacobian is always full rank due to the constraints in u_R shown in Table 1.

4.3 External Loop

The proposed control method is applied when the controlled variables are (generalised) velocities. In practical applications the command is in position or attitude, so an outer loop is needed. Assuming that the internal loop behaves like a controlled 2^{nd} order, as shown in Fig. 4, the outer controller can be synthesised with the linear control theory: a P or PI could be sufficient, root locus, LQR and so on. Note that the control actions given in (29) and (40)

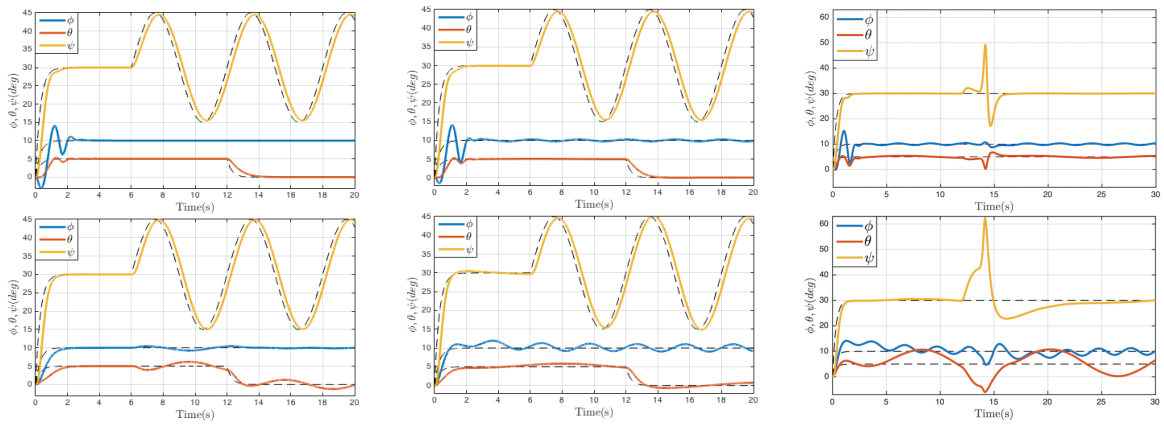

(a) Nominal Plant (b) Torque Disturbance (c) Uncertainty and Disturbance

Fig. 5. System response for three simulation scenarios. Top: Adaptive Control. Bottom: Baseline PID Controller. The black dashed lines represent the commands.

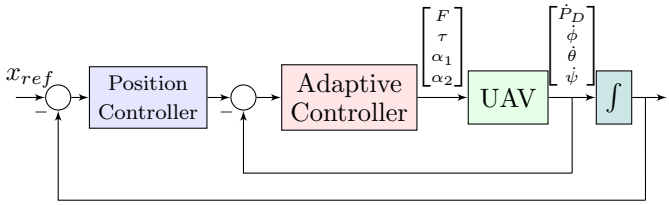

Fig. 6. Double Loop Control Scheme.

requires the derivative of the command $\dot{x}_C$, which can be easily given by the outer controller.

4.4 Disturbance Sources

The disturbance sources can be divided in uncertainties and external actions; the former deal with the approximated knowledge of the system, while the latter are due to the environment. For example, re-write (43) supposing that only an estimation of the mass, $\hat{m}$ and of the control action, $\hat{F}_x$ is known:

$$\begin{cases} \dfrac{d}{dt}v_x = \dfrac{1}{m}F_x + (r \cdot v_y - q \cdot v_z) \\ m = \hat{m} + \Delta m \\ F_x = \hat{F}_x + \Delta F_x \end{cases} \tag{47}$$

The dynamic system is rewritten again as:

$$\begin{aligned} \frac{d}{dt}v_x &= \frac{1}{\hat{m} + \Delta m}(\hat{F}_x + \Delta F_x) + (r \cdot v_y - q \cdot v_z) \\ &= \frac{1}{\hat{m}}\hat{F}_x + D_{unc} + D_{flex} + D_{coupling} + D_{ext} \end{aligned}$$

Where $D_{unc} = \frac{\Delta F_x - \frac{\Delta m}{\hat{m}}\hat{F}_x}{\hat{m}+\Delta m}$ represents the uncertainties due to Δm and ΔF_x, D_{flex} deals with the flexibility terms, $D_{coupling}$ considers the channels interaction and D_{ext} is an external acceleration due to wind gusts or interactions with the external environment.

5. SIMULATION RESULTS

The effectiveness of the proposed control system is demonstrated through non-linear simulations. The UAV parameters used in simulations are taken from the prototype and shown in Table 1. The controlled variables are the Euler angles η with initial condition $\eta_0 = [0\ 0\ 0]^T$. Moreover, a null-loop on $\dot{P}_D$ is built in order to concentrate the effort on the attitude. The desired commands is the following:

$$\phi_C = 10\,\text{deg},\ \theta_C = \begin{cases} 5\,\text{deg} & t \le 12 \\ 0\,\text{deg} & t > 12 \end{cases},\ \psi_C = \begin{cases} 10\,\text{deg} & t \le 6 \\ 0\,\text{deg} & t > 6 \end{cases}$$

The control parameters are tuned as follows; the adaptive coefficients are all set as $\eta_1 = \eta_2 = 2$, and the proportional gain are $[\alpha_{\dot{P}_D}\ \alpha_\phi\ \alpha_\theta\ \alpha_\psi] = [5\ 6\ 6\ 6]$. For all channels the outer loop is a simple P controller with gain $[k_\phi\ k_\theta\ k_\psi] = [2\ 2\ 4]$. The number of neurons used is 9, the RBF centers μ_i are evenly spaced in $[-1\ 1]$, and the widths σ_i are all 0.25. The performances are compared with a standard PI controller for the velocity, while the outer loop is the same.

Table 1.
UAV
Data

Parameter	Symbol	Value
Mass $[Kg]$	m	0.590
Inertia Matrix $\left[Kg \cdot m^2\right]$	I_B	$10^{-6}\begin{bmatrix} 3393.0 & 6.0 & -6.9 \\ 6.0 & 3918.3 & 47.1 \\ -6.9 & 47.1 & 2745.9 \end{bmatrix}$
Offset distance $[m]$	d_V	$8.572 \cdot 10^{-3}$
Force range $[N]$		$F \in [0.6818\ \ 7.6542]$
Torque range $[N \cdot m]$		$\tau \in [-0.0352\ \ 0.0352]$
Angle range $[rad]$		$\alpha_1, \alpha_2 \in \left[-\frac{\pi}{4}\ \ \frac{\pi}{4}\right]$
Motors time constant $[s]$	τ_m	0.175

5.1 Numerical results

The performance of the controller with the nominal plant is shown in Fig. 5a. As shown, the adaptive control system is much more decoupled and stable than the PI controller in the nominal case.

In the second simulation, to check the disturbance rejection, a time-varying torque disturbance is added in the attitude channels. The total disturbance is shown in Fig. 7 and it is composed by a fixed term plus a time-varying disturbance. Fig. 5b shows that the angles error based on the proposed method is much more limited, about ± 0.4 degrees than the PI method which has an error of about ± 2 degrees.

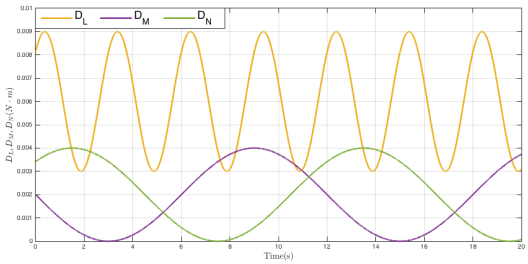

Fig. 7. Torque disturbance.

The simulation results confirm that the proposed approach effectively copes with the external disturbances and model uncertainties. Moreover, the performance comparison shows that the proposed outperforms over the standard PI controller.

In the third simulation a fault simulation is proposed: at $t = 12$ the UAV Inertia matrix becomes the 30% of the original one and a huge torque disturbance is added to the yaw channel: from Fig. 5c the proposed control method works way more better that the PI control and it can recover easily the steady state condition after the fault.

6. CONCLUSION

In this paper, an on-line adaptive control scheme is developed for a Spherical UAV in the presence of model uncertainties and external disturbances. The disturbance observer is designed based on a RBF-NN and the stability is proven using the Lyapunov control theory. Numerical simulation results confirms that the proposed control method is simple, easy to implement and quite effective. Further extensions include real test simulations, the application of the proposed control scheme on different platforms and the demonstration of the proposed control law in case of time-varying disturbances.

REFERENCES

Dixon, R. and Fernandez, Y. (2013). *Design of a Spherical UAV for Operations in Complex Environments*. Master's thesis, Cranfield University.

Gui, H. et al. (2015). Attitude control of spherical unmanned aerial vehicle based on active disturbance rejection control. In *34th Chinese Control Conference*, 1191–1195.

Lavretsky, E. and Wise, K. (2012). *Robust and Adaptive Control: With Aerospace Applications*. Advanced Textbooks in Control and Signal Processing. Springer.

Mizutani, S. et al. (2015). Proposal and experimental validation of a design strategy for a uav with a passive rotating spherical shell. In *IEEE/RSJ IROS 2015*, 1271–1278.

Stevens, B., Lewis, F., and Johnson, E. (2015). *Aircraft Control and Simulation: Dynamics, Controls Design, and Autonomous Systems*. Wiley.

Appendix A. NL-MIMO-AC, POSITION

The relation between v_B and v_E is (9). Deriving the inverse of (9) it holds

$$\dot{v}_B = D\dot{C}Mv_E + DCM\dot{v}_E \tag{A.1}$$

Substituting (A.1) in (41) and expliciting $\dot{v}_E$ yields

$$\begin{aligned}\frac{d}{dt}v_E = {} & DCM^T\frac{1}{m}\mathbf{F} - DCM^TD\dot{C}Mv_E + \dots \\ & -DCM^T(J^{-1}\dot{\eta}) \times (DCMv_E) - [0\ 0\ g]^T\end{aligned} \tag{A.2}$$

Equation (A.2) is in form (38), where

$$f = -DCM^TD\dot{C}Mv_E - DCM^T(J^{-1}\dot{\eta}) \times (DCMv_E) \tag{A.3}$$

$$D = -[0\ 0\ g]^T \tag{A.4}$$

And the map $g = DCM^T\frac{1}{m}$ has always $rank = 3$.

Appendix B. NL-MIMO-AC, ATTITUDE

The relation between ω and η is (8). Deriving the inverse of (8) it holds

$$\dot{\omega} = (\frac{d}{dt}J^{-1})\dot{\eta} + J^{-1}\ddot{\eta} \tag{B.1}$$

Where

$$\frac{d}{dt}J^{-1} = \begin{bmatrix} 0 & 0 & -c_\theta\dot{\theta} \\ 0 & -s_\phi\dot{\phi} & c_\phi c_\theta\dot{\phi} - s_\phi s_\theta\dot{\theta} \\ 0 & -c_\phi\dot{\phi} & -s_\phi c_\theta\dot{\phi} - c_\phi s_\theta\dot{\theta} \end{bmatrix} \tag{B.2}$$

Substituting (B.1) and (8) in (42) and expliciting $\ddot{\eta}$ yields

$$\frac{d}{dt}\dot{\eta} = JI_B^{-1}T - J\left((\frac{d}{dt}J^{-1})\dot{\eta} + I_B^{-1}\left((J^{-1}\dot{\eta}) \times (I_BJ^{-1}\dot{\eta})\right)\right) \tag{B.3}$$

Equation (B.3) is in the form (38), where

$$f(\eta,\dot{\eta}) = -J\left((\frac{d}{dt}J^{-1})\dot{\eta} + I_B^{-1}\left((J^{-1}\dot{\eta}) \times (I_BJ^{-1}\dot{\eta})\right)\right) \tag{B.4}$$

$$g(\eta,\dot{\eta}) = JI_B^{-1} \Rightarrow g^{-1} = I_BJ^{-1} \tag{B.5}$$

Note that $rank\ g^{-1} = 3$ is ensured if $\theta \neq \pm\frac{\pi}{2}$ and the inertia matrix I_B is diagonal; the condition must be checked in all the other cases.